



SEISMIC RESPONSE OF COMPOUND STEEL COLUMNS WITH PARTIALLY-RESTRAINED EXPOSED BASE-PLATE CONNECTIONS

G. Della Corte⁽¹⁾, G. Sarracco⁽²⁾, R. Landolfo⁽³⁾

⁽¹⁾ Associate Professor, University of Naples Federico II, gdellaco@unina.it

⁽²⁾ Research fellow, University of Naples Federico II

⁽³⁾ Full Professor, University of Naples Federico II, landolfo@unina.it

Abstract

This paper describes a comparison of experimental results and theoretical predictions regarding the lateral force-displacement response of compound steel columns with partially-restrained exposed base-plate connections.

Two specimens were fabricated and tested, to represent samples of real columns extracted from an existing industrial building. Both columns were made of two I-shaped profiles connected by means of battens, but with significant differences in the scheme of battening from one specimen to the other. The base plate connections also were significantly different from one case to the other, in terms of both design concept and local detailing.

Preliminary tests were carried out in the elastic range of response, under varying levels of applied axial force. Such elastic tests were used to measure variations of the initial stiffness and corresponding yield displacements with the applied axial force. Subsequently, a cyclic loading test was carried out, per each specimen, to investigate the inelastic response. The plastic mechanisms, ductility, and energy dissipation capacity of the two specimens, as resulting from the experimental tests, are firstly described and commented.

Subsequently, detailed finite-element models were developed for both specimens using the ABAQUS software. After describing the essential features of the numerical models, a comparison of theoretical predictions with experimental results is illustrated and discussed.

Keywords: Columns, connections; cyclic response; ductility; steel structures.



1. Introduction

Industrial steel buildings sometimes comprise compound columns, where two I-shaped profiles are connected together to form one single column. Due to flexibility of connections between the two profiles, the response of a compound column is frequently represented as the response of a single member with significant shear deformations along with bending deformations [1]. Besides, such columns are usually connected to a concrete foundation by means of steel base plates and anchor rods or bolts. The response of the base-plate connection also strongly affects both the elastic and inelastic response of the whole system, because of the significant contribution to the system elastic flexibility and involvement into the plastic mechanism due to the large size of column members (semi-rigid and partial-strength connections). Such industrial buildings, when located in seismic areas, have been frequently designed in the past with minor consideration of inelastic response. Two causes might be at the origin of this situation: 1) load combinations other than the seismic one governed design; 2) at the design stage, there was lack of specific design rules or guidance for seismic response. In addition, seismic hazard at the structure site might have been underestimated in the past, due to lack of specific knowledge. Therefore, due to either one of the previous issues or because of a combination of factors, damage to the base connections might be significant [2], [3]. Experimental test results and analytical models for single columns with unstiffened base plates are currently available in the technical literature (e.g., among recently published work, [4], [5]). Design rules are also available to evaluate resistance of column base plate connections under combinations of axial forces and bending moments ([6], [7]). Eurocode 3 (EC3) [7] provides rules to calculate also the initial (elastic) rotational stiffness, although performance of the method is still worthy of investigation [8], especially in case of design concepts and detailing rules used in the past prior to the code development.

Within a previous theoretical study on seismic risk assessment of an industrial steel building [9], two types of existing compound columns and relevant exposed base-plate connections were identified. Subsequently, full-scale specimens were fabricated and tested, replicating the existing structures as close as possible. This paper describes firstly the experimental lateral loading tests and, secondly, numerical finite element modelling and relevant comparison with experimental results.

2. Specimens and test set-up

Figure 1 illustrates the essential geometry of specimens. Specimen 1 (Fig. 1a) comprises two I-shaped profiles (IPE 360) with battens made of plates welded to the flanges of the IPE shapes. The IPE 360 profiles were both welded to a single base plate, which was stiffened with vertical plates as shown in the figure. Then, the column was anchored to a concrete foundation by means of 4 steel rods. Specimen 2 (Fig. 1b) was also obtained by the assembling of two I-shaped profiles (IPE 600), but with battens obtained in this case by cutting I-shaped pieces from a HE 500 A profile. The two flanges of each HE 500 A piece were then bolted to the two webs of the main IPE 600 profiles. Each of the two IPE 600 profiles was welded to a different stiffened base plate. In the original design (i.e., in the original compound column from the existing industrial building), three anchor rods per each of the two base plates were included, as shown in Figure 1(b). However, for these tests and due to limitations to the horizontal load actuator capacities, nuts were not used for the anchor rods in the middle position at each row of anchors. This allowed retaining the shear sliding force capacity, while reducing the total bending moment capacity and without changing the qualitative response (based on theoretical expectations). Besides, this solution allowed also comparing more clearly response of specimen 1 and specimen 2, which were expected to have similar moment capacities with this solution. Figure 1 also shows a baseline below the columns, indicating the top surface of a RC block used to simulate in the laboratory the real column foundation. Geometry of the foundation block is not reported here, because it is unessential. A gap joint was designed between the steel column and the RC foundation block, in order to allow for the correct positioning of the steel column. The design value of this gap was 50 mm; the actual mean value was only marginally modified during the assembling of the specimens in the laboratory. In both cases, the foundation anchors were rods, with nominal diameter equal to 30 mm and a threaded portion at each end (pitch of the helicoid threading equal to approximately 1 mm).

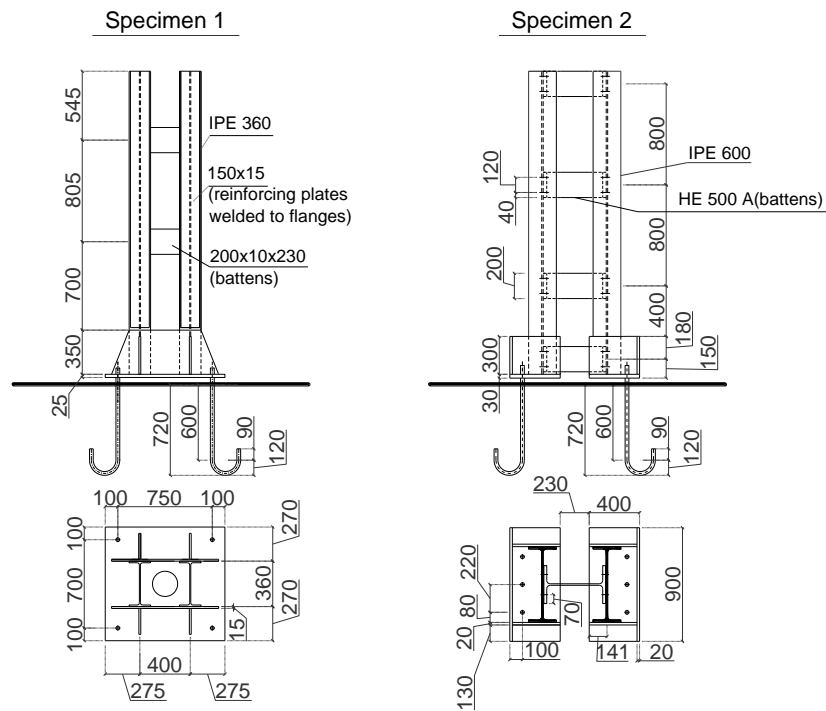


Fig. 1 – Geometry of specimens

2.1 Test set-up for specimen 1

Figure 2 shows the test set-up in case of specimen 1. A horizontal load actuator applied lateral forces at the column tip. The horizontal load actuator was connected to a transverse beam, which distributed the load to two longitudinal beams. These longitudinal beams were pin connected to the four flanges of the two IPE shapes comprising the compound column. The pin connections allowed avoiding the introduction of additional shear connection of the two IPE profiles. Besides, a couple of vertical loading jacks introduced a vertical load into the specimen. These vertical loading jacks were placed on the top of a transverse beam. Reaction to the vertical loading jacks was obtained by means of vertical ties, which were connected to a steel beam anchored the laboratory strong floor. Figure 2 shows also horizontal ties (at the level of the strong floor), used to equilibrate horizontal force components generated by inclination of the vertical ties following the horizontal displacement of the column tip. It is noted that a pin connection was used at both the bottom and top ends of the two vertical ties. The reinforced concrete block simulating the column foundation was anchored to the laboratory strong floor by means of anchoring bars which were pre-stressed to eliminate the danger of foundation overturning. Figure 2 shows also (in the longitudinal section only) the arrangement of displacement sensors (DSs). Both vertical (V) and horizontal (H) displacements were measured. Generally, the use of inductive sensors (i.e. LVDTs, truncated to LT in Figure 2) was preferred. However, due to limitations to the number of available sensors, some potentiometer sensors (string potentiometers, SP in Figure 2) were also included in the test setup. In Figure 2, the sensor displacement nominal capacity is also reported, measured in mm (for instance ± 250 indicates a total displacement capacity of 500 mm). When possible, two DSs at the same height were placed symmetrically and the mean value of the measured displacement was adopted to characterize the specimen displacement at that level. Additional to horizontal column displacements and vertical base plate and anchor displacements, shear deformations of battens were also estimated by measuring angle changes between the column flange and battens (B).

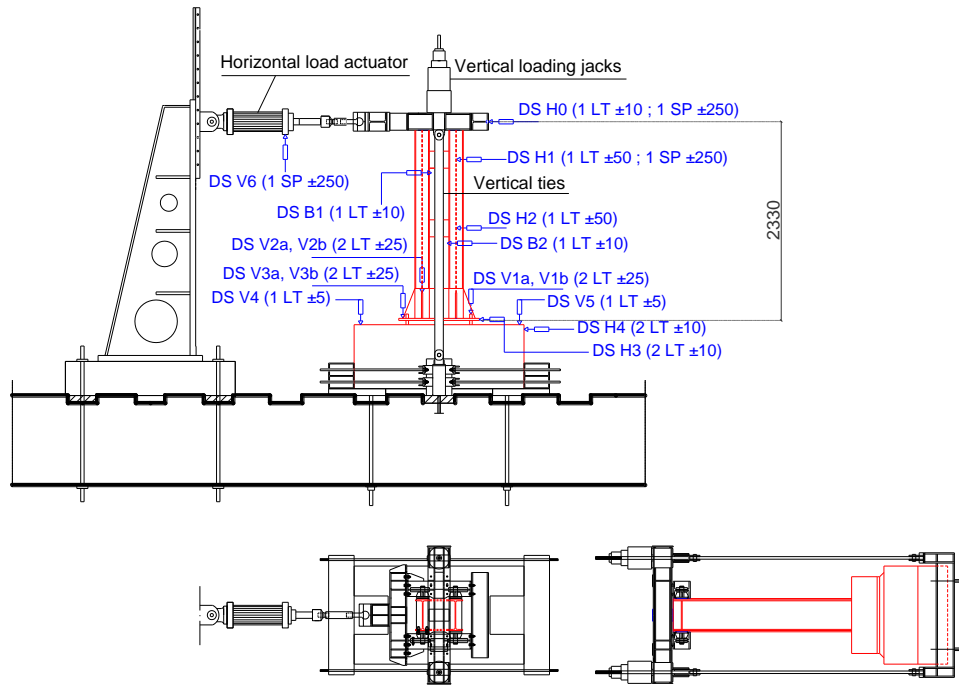


Fig. 2 – Specimen 1: test set-up

2.2 Test set-up for specimen 2

The test set-up for specimen 2 is similarly illustrated in Figure 3. Load application, both horizontal and vertical, was done in the same manner as for specimen 1. Differences were needed in terms of placement of DSs, because of the different characteristics of the two specimens. The arrangement of DSs in case of specimen 2 is shown in Figure 3 using a nomenclature similar to that already described for specimen 1 (H stands for horizontal and V for vertical displacements).

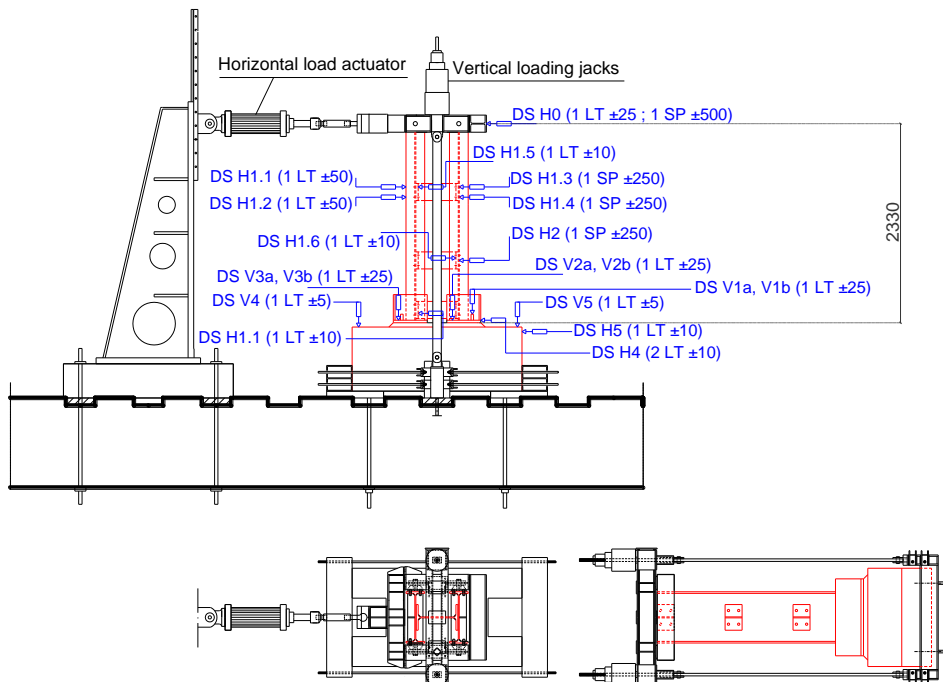


Fig. 3 – Specimen 2: test set-up

3. Test results

Both monotonic and cyclic loading tests were carried out, for both specimens. Monotonic loading tests had two purposes: 1) to measure the initial (elastic) stiffness, and 2) to evaluate the effect of the level of axial force on the initial stiffness. For the latter purpose, multiple levels of axial force were applied. Interested readers are referred to a preceding paper for more details [10]. Only cyclic loading tests are further described in the following.

In the cyclic tests, the axial force externally applied onto columns was equal to 150 kN. The cyclic loading protocols were defined in accordance with ECCS [11] (displacement amplitudes increased as integer multiples of the yield displacements, with 3 repetitions per each amplitude). Yield displacements were calculated using the measured initial stiffness from the monotonic loading tests and a theoretical prediction of the plastic resistance [10]. Figure 4a shows the resulting cyclic loading protocols, for both specimen 1 and specimen 2, in terms of drift angle, i.e. the ratio between the displacement applied at the column tip and its distance from the bottom face of the column base plate, $h = 2330$ mm, Figures 2 and 3). Figure 4b shows results from tension tests on steel specimens representing the behavior of the anchor rods. The steel mean yield strength was equal to approximately 400 MPa. Tests were also carried out on the mortar (“Mapefill”, provided by Mapei) used to fill the gap between the RC foundation block and the steel base plate. These mortar tests were carried out adopting the recommendations of the European standard EN 12190 [12]. Figure 4c reports results from the compression tests on the mortar specimens from the column assembly 1. Similar results were obtained in case of the column assembly 2 (Fig. 4d). The compression tests showed average mortar compression strength equal to 48 MPa and 50 MPa, approximately, for the column assemblies 1 and 2 respectively. Strength of the concrete used for the foundation blocks was also tested using three cubic specimens per each of the column assemblies. The concrete mean compression strength was equal to 46 MPa (concrete of the two foundation blocks was cast at the same time).

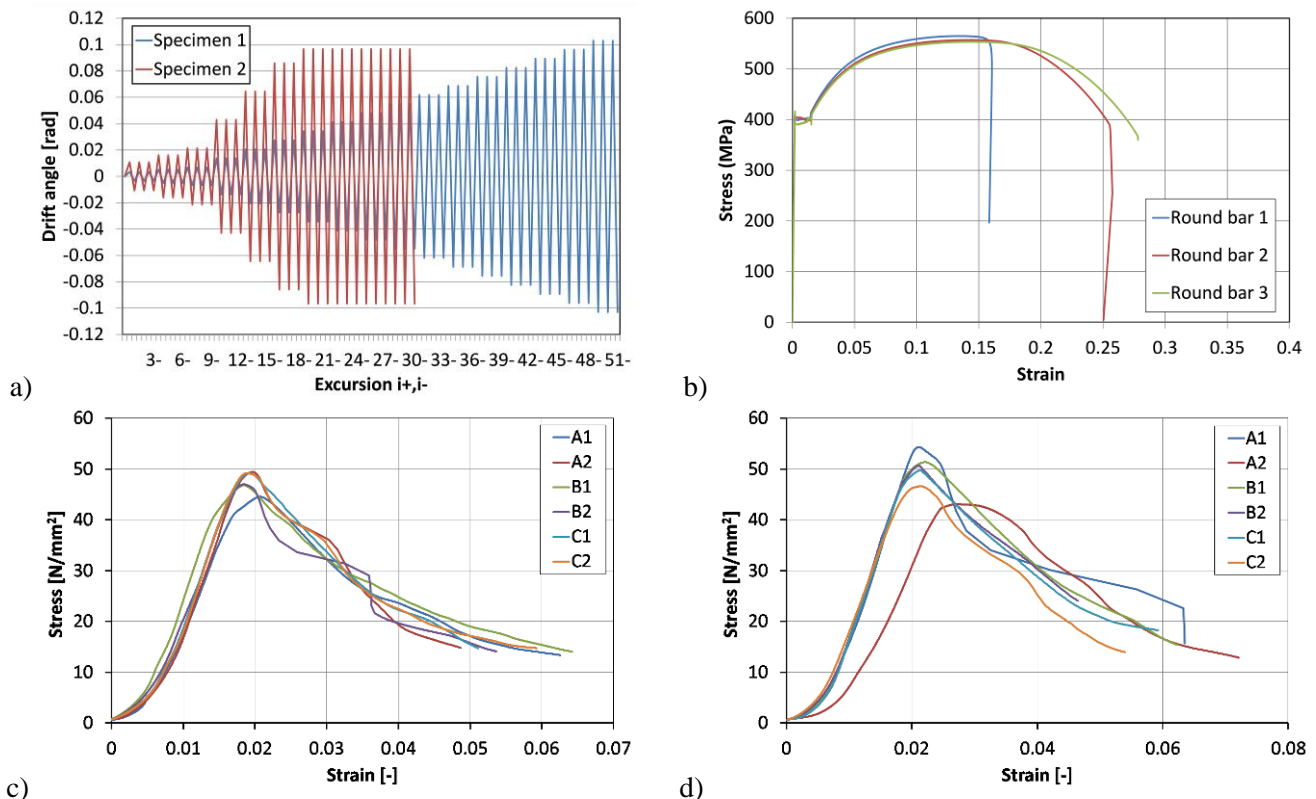


Fig. 4 – Cyclic loading protocols (a) and qualification tests on materials (b, c and d)

3.1 Cyclic loading test results - Specimen 1

Figure 5a illustrates the hysteresis response of specimen 1, in terms of column base moment versus drift angle. There is strong pinching of hysteresis loops, due to the continually opening and closing of a gap between the base plate and mortar substrate on the tension side. The anchor rods and the base plate were highly deformed in the plastic range, as testified by results plotted in Figure 5b which refers to measures taken by DS V1 (Fig. 2). Figure 5c refers to vertical displacements measured on the compression side, close to the plate edge. The figure clearly shows that the mortar crushed at a certain point during the loading history, thus originating negative (i.e. downwards) displacements of the base plate. Figure 5d shows the equivalent viscous damping (EVD) ratio calculated per each cycle of imposed deformation. In the elastic range of response (i.e. for a drift angle smaller than approximately 0.01 rad), the equivalent damping ratio is close to 2%, while values as high as 6%-8% were obtained for large inelastic drift angle demand. Plastic deformations of the base plate and anchors, as well as crushing of mortar and ultimate fracture of one anchor rod, are illustrated in Figure 6.

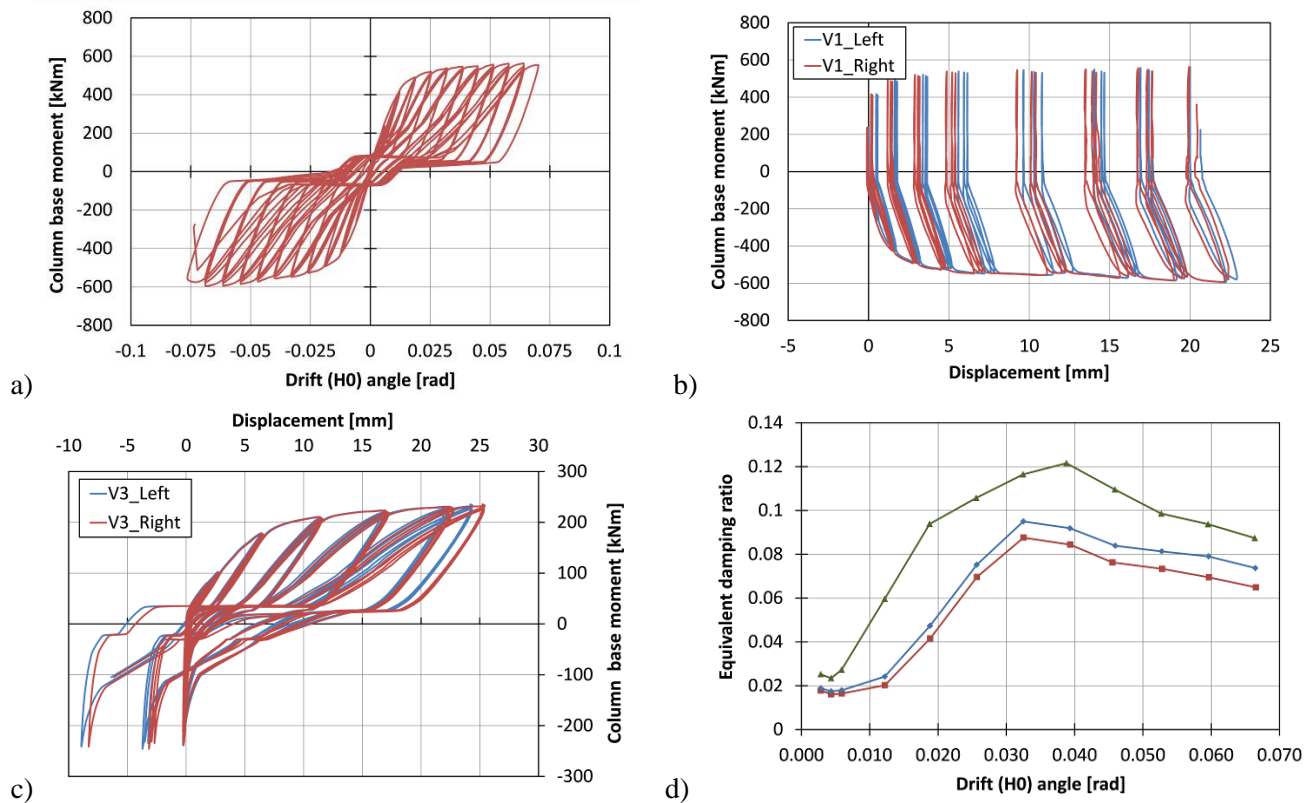


Fig. 5 – Specimen 1: a) Base moment vs. drift angle; b) tension-side response; c) compression-side response; d) equivalent damping ratio.

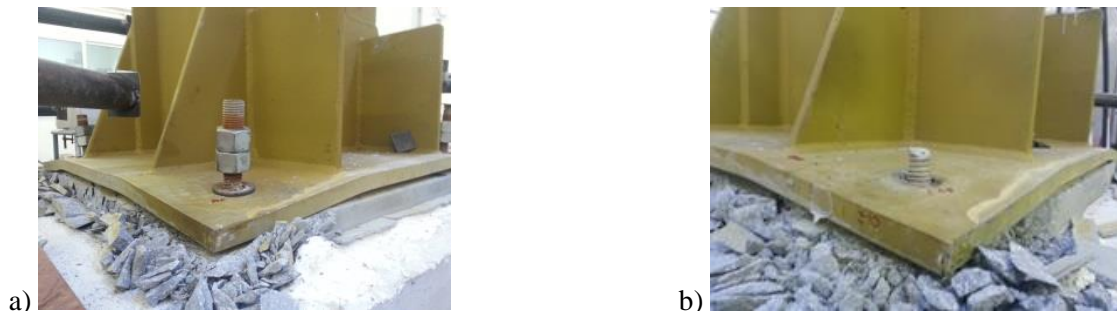


Fig. 6 – Specimen 1: a) plastic deformations of base plate and anchors; b) fracture of one anchor.

3.2 Specimen 2

Figure 7a illustrates the column base moment vs. drift angle response of specimen 2. The maximum displacement capacity of the load actuator was reached in this test, corresponding to a peak drift angle equal to approximately 0.09 rad. Plots provided in Figures 7b and 7c illustrate the local response of the column base connection by reporting vertical displacements on the tension side (Fig. 7b) and compression side (Fig. 7c). Finally, Figure 7d shows the EVD ratio. In the elastic range of response (i.e., for a drift angle smaller than approximately 0.02 rad, in this case) the EVD ratio is slightly larger than 2%. Subsequently, the EVD ratio increases steadily, reaching values as high as 10% at the maximum drift angles (0.09 rad, approximately).

Figure 8 illustrates a couple of photographs taken during the test. Essentially, the behavior of this specimen can be described as made of two phases. In the first phase, the shear coupling of the two IPE 600 profiles is effective and the system behaves essentially as a single piece (Fig. 8a), although with significant global shear deformations of the compound column. The second phase takes place after yielding of the (relatively weak) moment connection between the battens and the column web panel, and essentially consist of the two column profiles behaving as independent members for any incremental load (Fig. 8b). The second phase of response was dominating for larger displacement amplitudes, because of the relatively small plastic moment resistance of the battens' connections. Figure 8 shows that there was no crushing of the mortar and no significant plastic deformation of the base plate, while significant plastic deformations were located in the anchors.

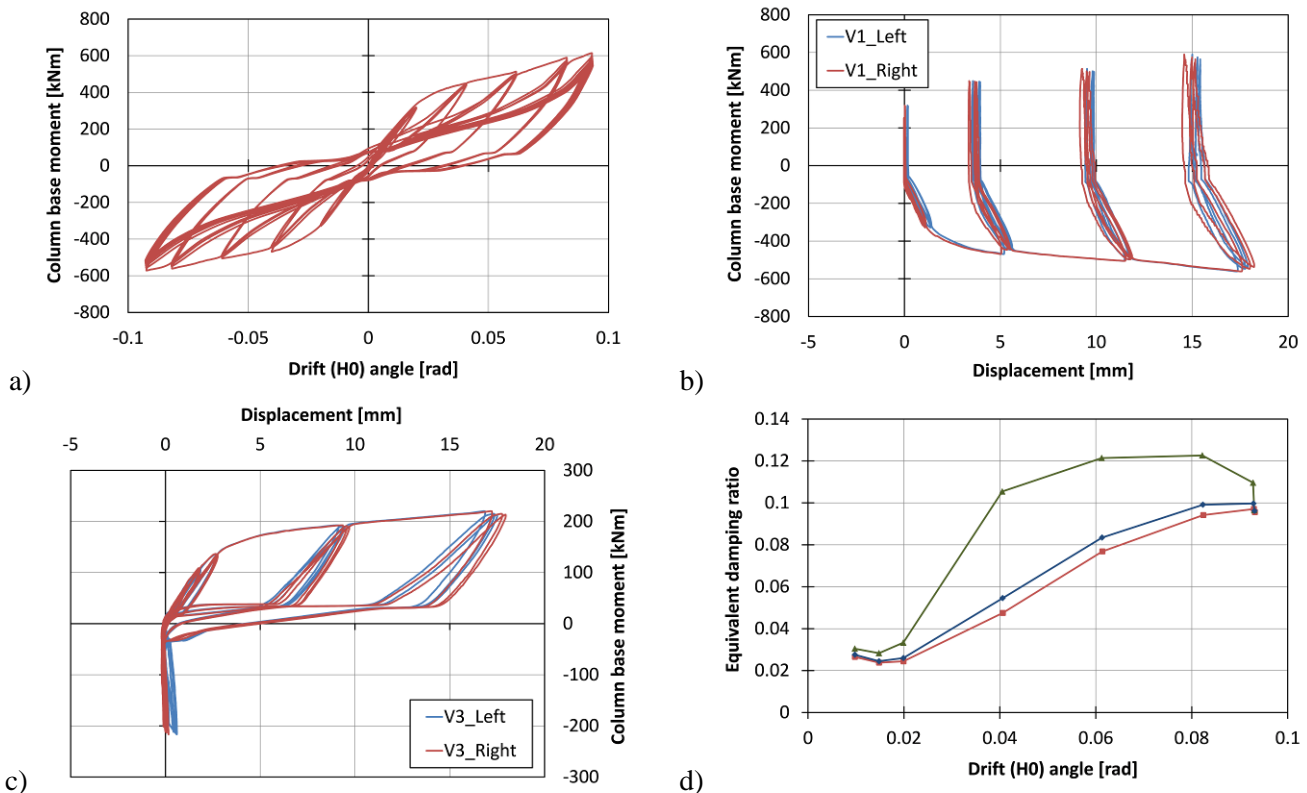


Fig. 7 – Specimen 2: a) Base moment vs. drift angle; b) tension-side response; c) compression-side response; d) equivalent damping ratio.

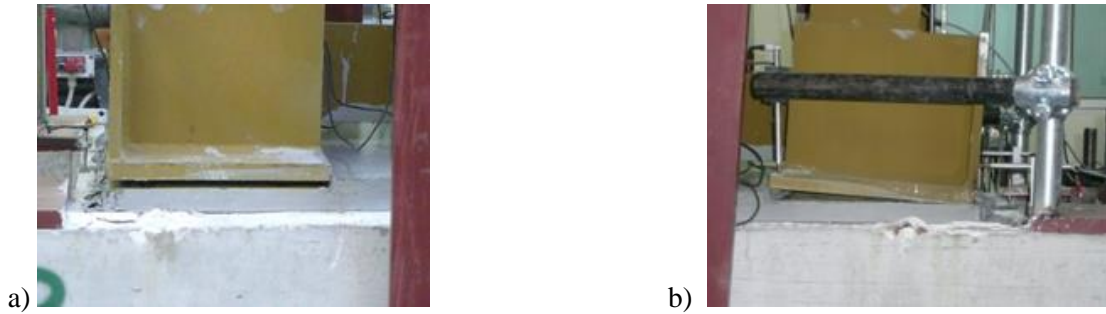


Fig. 8 – Specimen 2: a) Phase 1 behavior; b) Phase 2 behavior.

4. Finite element models

The general purpose finite element (FE) software ABAQUS [13] was adopted to carry out numerical analyses of both specimens. Considering that the specimens are both doubly symmetric, half-models were built up as shown in Figure 9.

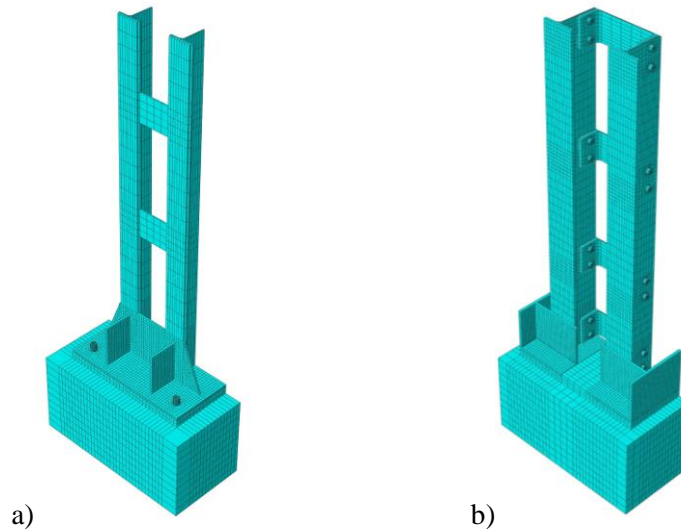


Fig. 9 – Finite element models of specimen 1 (a) and specimen 2 (b)

All the parts comprising the models were meshed with first order linear reduced integration hexahedral elements (C3D8R). As it is well known, this type of finite element is affected by hour-glassing; therefore, an adequately fine mesh (i.e., at least two elements through the thickness of a plate) and the artificial hourglass stiffness were adopted to provide acceptable results. Element distortion was reduced by increasing the local mesh density along the edges of circular parts and holes, and generally where stress concentrations were expected (or verified) to occur. The final mesh density was checked by means of sensitivity analyses.

4.1 Material properties and response

Material properties were based on the laboratory tests previously mentioned for the anchors, while information provided by the manufacturer was used for the base plates and column profiles. Table 1 provides information about the main steel properties for the base connection plates and the column profiles, in terms of yielding (f_y) and ultimate (f_u) stresses, as well as ultimate strains (ϵ_u).



Table 1 – Mechanical properties of steel plates and profiles

Item	f_y (MPa)	f_u (MPa)	ϵ_u (%)
Plate 25 mm	301	474	30.2
Plate 30 mm	301	474	30.2
IPE 360	289	429	37.5
IPE 600	320	461	38.6
HE 500 A	389	487	26.7

The Von Mises yield criteria and the kinematic strain-hardening rule were adopted for all the steel parts.

The concrete and the mortar were modelled as frictional and pressure dependent Drucker-Prager materials. The unidirectional compressive behavior of the grout, including post failure behavior, was calibrated using the material tests described in section 3. The tensile strength was fixed at 1/10 of the maximum compressive strength (the value assigned to this property was checked to have negligible effects on the model response). Parameters of the tri-axial stress response were fixed using values taken from the literature for concrete [14].

Interactions between different parts were modelled by means of surface-to-surface contact with normal behavior defined as “hard” contact and allowing separation. The tangential behavior was frictionless except for the base plate and grout, where an isotropic friction formulation was adopted with a constant friction coefficient of 0.45 [15], [16].

4.2 Boundary conditions and analysis procedure

The bottom section of the foundation block was fixed in the space, since the experimental evidence highlighted the absence of any significant displacements. The FE model described in this paper did not include hooks of foundation anchors, while it was assumed that a fixed restraint can be considered at the end of the anchors’ straight portion (i.e., any deformation of the anchoring system is neglected below the mentioned terminal cross section of the anchors). Further information regarding this assumption and its consequences is provided in the following.

The column axial force and lateral displacements were controlled using a master joint at the column top cross section. Displacement control was adopted, following the displacement measured by sensor H0 (Figs. 2 and 3). Numerical analyses accounted for geometrical non-linearity.

5. Numerical results and comparison with the physical experiments

The following sections illustrate results from the numerical analysis as well as comparison with the experimental results. Discussion is separately addressed for specimen 1 and specimen 2.

5.1 Specimen 1

Figure 10 shows numerical results from analysis of the FE model of specimen 1. Figure 10a reports the global hysteresis response in terms of applied horizontal force vs. displacement at the tip of the column. Figure 10b shows the local connection response in terms of applied horizontal force vs. vertical displacement at the tip of the anchors. Figure 10c illustrate the local connection response in terms of applied horizontal force vs. vertical displacement at one edge of the column base plate. In the above figures, experimental results are also reported to make a direct comparison. Finally, Figure 10d shows the predicted plastic mechanism from the numerical model, which can be compared to the plastic deformations observed during the experimental tests and illustrated in Figure 6a. The theoretical vs. experimental agreement is generally good. From Figure 10a, one can see that some underestimation of displacements at given applied forces occurs when very large plastic deformations take place.

This could be explained by the inability of the model to capture completely the crushing of the mortar, as illustrated in Figure 10c, as well as to the absence in the model of the anchoring hooks.

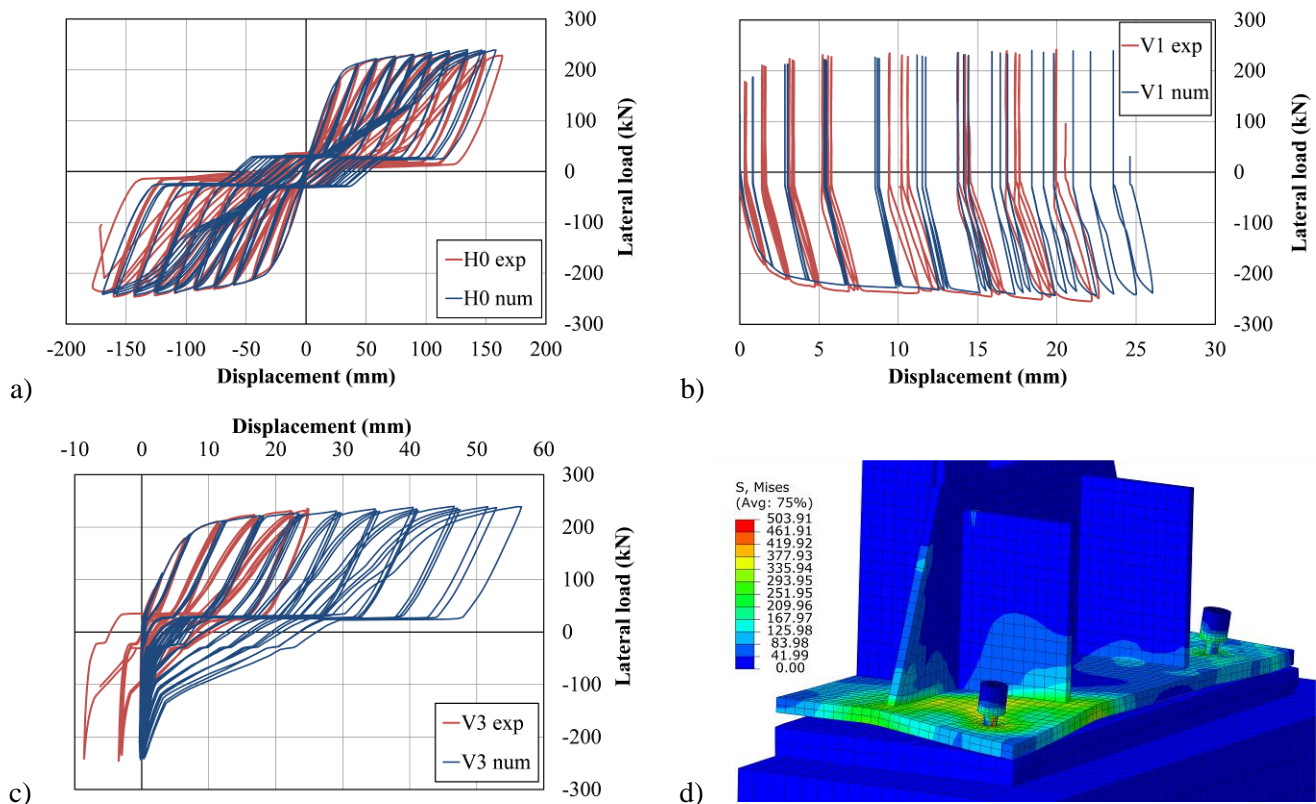


Fig. 10 – Numerical results for specimen 1: a) Base moment vs. drift angle; b) tension-side response; c) compression-side response; d) plastic deformations of base plate and anchors.

5.2 Specimen 2

Similar to Figure 10, Figure 11 compares results obtained from experimental and numerical cyclic loading tests, but for specimen 2. As described in section 4.2, specimen 2 exhibited large plastic deformations of foundation anchors and significant plastic deformations at the moment connections between the column web panel and the battens. Such plastic deformations are generally well captured by the numerical model, as illustrated for example in Figure 11d with reference to the column base. While for specimen 1 there was large and widespread crushing of the mortar at the column base, this was not observed for specimen 2. Accordingly, numerical results relevant to the plate edge, results shown in Figure 11c, are in good agreement with experimental observations. Similar to specimen 1, the tension-side response of the connection is reasonably well predicted by the numerical model (Fig. 11b). Therefore, the overall cyclic response of specimen 2 is also reasonably well predicted by the numerical model, as shown in Figure 11a. As mentioned in the preceding discussion, in case of specimen 2 the test had to be stopped due to the exceedance of the force actuator displacement capacity, prior to any form of abrupt failure. This occurred at a drift angle of approximately 0.09 rad (Fig. 7a). After this maximum displacement was reached, additional cycles of loading at constant displacement amplitude were carried out, to look for strength degradation. Slow degradation took place, as visible in Figure 11a (as well as in Figure 7a) after a careful look at the last portion of the hysteresis loops. Figure 11a shows that such degradation is not accounted for in the numerical model. Notwithstanding, considering the very large displacement demand, and the corresponding slow degradation of the specimen response, performance of the numerical model is considered sufficiently accurate to represent the seismic response of the investigated sub-assembly.

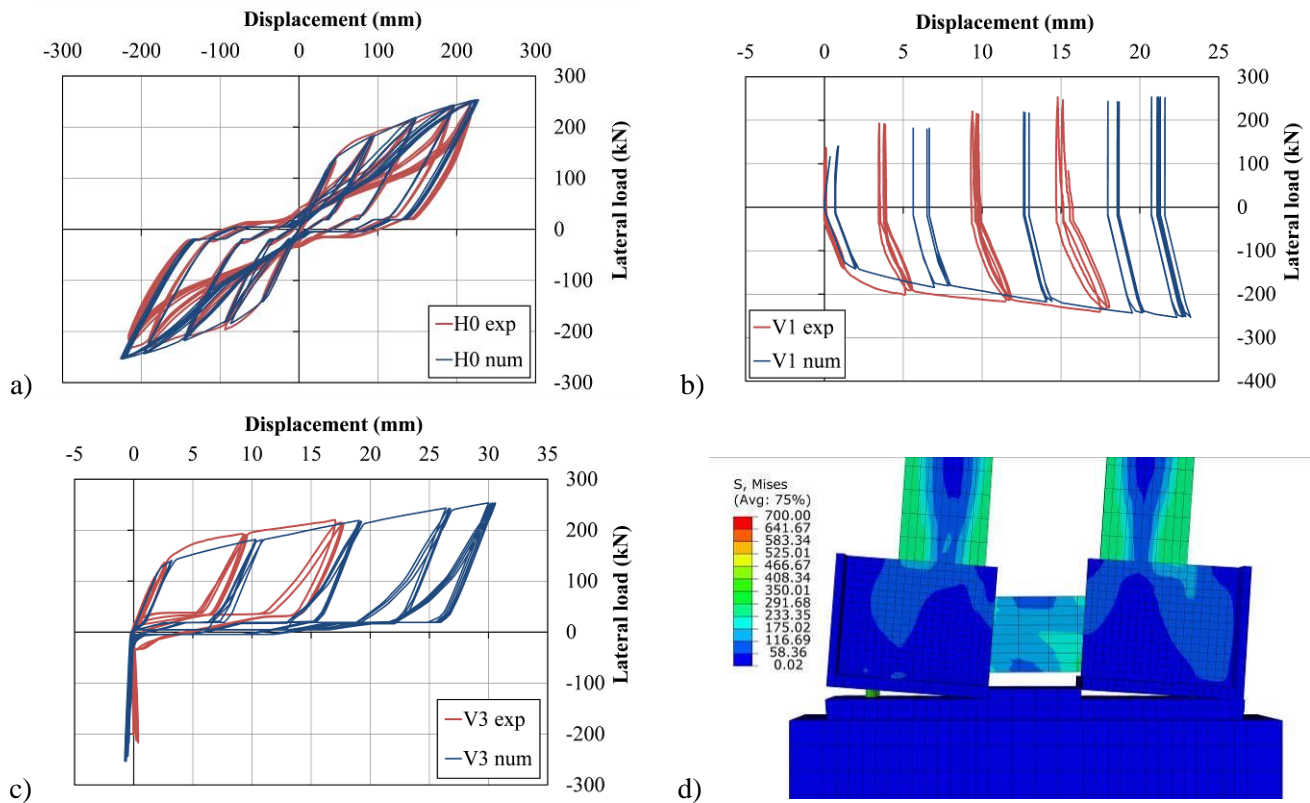


Fig. 11 – Numerical results for specimen 2: a) Base moment vs. drift angle; b) tension-side response; c) compression-side response; d) plastic deformations of anchors.

6. Conclusions

Experimental tests on two specimens representing samples of compound columns and relevant base connections were carried out, in order for investigating their seismic response by means of cyclic inelastic loading tests. The two compound columns differed for the type of shear connection and base connection. Specimen 1 was a relatively stiff column, with welded battens, and a single base plate connection. Inelasticity was located in the base connection, with a mixed plastic mechanism involving both the base plate and the foundation anchors. Specimen 2, was a more flexible column, with bolted moment-connections between the battens and the column web panels. Plastic deformations involved the anchors (tensile yielding with almost elastic base plate), and the (relatively weak) moment connections between the battens and the column web panels. In particular, yielding of the batten-to-column moment connections, occurring at relatively small lateral forces, and the subsequent tensile yielding of anchors transformed the compound column into a mechanism of two independent members. This kinematic behavior was favorable in terms of global displacement capacity, because it corresponded to smaller axial deformation demand to the anchors. In fact, specimen 2 was able to sustain a drift angle of approximately 0.09 rad without fracture of anchors, while specimen 1 failed by anchor fracture at a slightly smaller displacement demand.

Finite element modelling of both specimens was also carried out, and the numerical model predictions were compared to the experimental results. Generally, the numerical models have shown good agreement with the experimental results, especially at small-to-medium displacements. Further developments might consider improvements in modelling the grout mortar degradation at the column base, and eventually including the anchor hooks in the model. However, such phenomena had small effects only at large displacements (corresponding to drift angles larger than 0.05 rad in case of specimen 1 and 0.08 rad for specimen 2). Therefore, the ability of the numerical model to capture the experimental results is considered adequate.



7. Acknowledgements

This research was financially supported by the ReLUIIS consortium (Italian Network of Universities' Laboratories for research on Earthquake Engineering) under a grant provided by the Italian Department of Civil Protection (DPC). The financial contribution is gratefully acknowledged.

8. References

- [1] CEN–European Committee for Standardization (2005): *Eurocode 3: Design of steel structures – Part 1–1: General rules and rules for buildings*. EN 1993-1-1, Eurocode 3, Brussels.
- [2] Bertero VV, Anderson JC, Krawinkler H. (1994): Performance of Steel Building Structures during the Northridge Earthquake. *Report No. UCB/EERC-94/09*, Earthquake Engineering Research Center, University of California at Berkeley.
- [3] Grauvilardell JE, Lee D, Hajjar JF, Dexter RJ (2005): Synthesis of design, testing and analysis research on steel column base plate connections in high seismic zones. *Structural Engineering Report No. ST-04-02*, Department of Civil Engineering, University of Minnesota.
- [4] Kanvinde AM, Grilli DA, Zareian F (2012): Rotational stiffness of exposed column base connections: Experiments and analytical models. *Journal of Structural Engineering (ASCE)*, 138(5), 549-560.
- [5] Latour M, Piluso V, Rizzano G (2014): Rotational behaviour of column base plate connections: Experimental analysis and modelling. *Engineering Structures*, 68, 14-23.
- [6] Fisher JM, Kloiber LA (2006): Base plate and anchor rod design. *American Institute of Steel Construction (AISC) design guide 1, second edition*.
- [7] CEN–European Committee for Standardization (2005): *Eurocode 3: Design of steel structures – Part 1–8: Design of joints*. EN 1993-1-8, Eurocode 3, Brussels.
- [8] Della Corte G, Terracciano G, Landolfo R (2008): Review of experimental data on the moment rotation response of steel bolted end-plate beam-to-column joints. *Second European Conference on Earthquake Engineering and Seismology*, Istanbul, Turkey.
- [9] Della Corte G, Petruzzelli F, Iervolino I (2013): Structural modelling issues in seismic performance assessment of industrial steel buildings. *4th Thematic ECCOMAS Conference on Computational Methods in Structural Dynamics and Earthquake Engineering*, Kos, Greece (Paper ID 1461).
- [10] Della Corte G, Landolfo R (2015): Experimental tests of compound columns and their base-plate connections subject to axial and horizontal forces. *Eight International Conference on Advances in Steel Structures*, Lisbon, Portugal.
- [11] ECCS–European Convention for Constructional Steelwork (1986): *Recommended testing procedure for assessing the behaviour of structural steel elements under cyclic loads*. Technical Committee 1, TWG 1.3—Seismic Design, Publ. No. 45.
- [12] CEN–European Committee for Standardization (2000): *EN 12190 Products and systems for the protection and repair of concrete structures – Test methods – Determination of compressive strength of repair mortar*. Bruxelles, Belgium.
- [13] Hibbitt, Karlsson and Sorensen (2012): *ABAQUS Analysis User's Manual, Version 6.12*. Dassault Systèmes Simulia Corp., Providence, RI, USA.
- [14] Lubliner J, Oliver J, Oller S, and Oñate E (1989): A Plastic-Damage Model for Concrete. *International Journal of Solids and Structures*, 25(3), 229–326.
- [15] Jaspart JP, Vandegans D. (1998): Application of the component method to column bases. *Journal of Constructional Steel Research*, 48, 89–106.
- [16] Kanvinde AM, Jordan SJ, Cooke RJ (2013): Exposed column base plate connections in moment frames - Simulations and behavioral insights. *Journal of Constructional Steel Research*, 84, 82–93.